Food Hydrocolloids 142 (2023) 108849

Contents lists available at ScienceDirect

Food Hydrocolloids

journal homepage: www.elsevier.com/locate/foodhyd

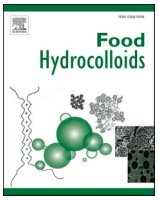

Development and characterization of walnut oleogels structured by cellulose nanofiber

Xiufen Li [a,c,1], Guanshui Guo [a,c,1], Yuxuan Zou [a,c], Jia Luo [b,*], Jun Sheng [d,**], Yang Tian [a,c,***], Jienan Li [e]

[a] College of Food Science and Technology, Yunnan Agricultural University, 425 Fengyuan Road, Kunming, 650201, Yunnan, People's Republic of China
[b] Kunming Branch, CAS Key Laboratory of Tropical Plant Resource and Sustainable Use, Xishuangbanna Tropical Botanical Garden, Chinese Academy of Sciences, 88 Xuefu Road, Kunming, 650223, Yunnan, People's Republic of China
[c] Engineering Research Center of Development and Utilization of Food and Drug Homologous Resources, Ministry of Education, Yunnan Agricultural University, 425 Fengyuan Road, Kunming, 650201, Yunnan, People's Republic of China
[d] Key Laboratory of Pu-er Tea Science, Ministry of Education, Yunnan Agricultural University, 425 Fengyuan Road, Kunming, 650201, Yunnan, People's Republic of China
[e] Yunnan Institute of Medical Device Testing, 616 Kefa Road, Kunming, 650101, Yunnan, People's Republic of China

ARTICLE INFO

Keywords:
Oleogels
Cellulose nanofibers
Emulsion-templated method
Walnut

ABSTRACT

Edible oleogels were successfully prepared by cellulose nanofibers (CNFs) as the unique oleogelator through emulsion-templated method at varying CNF concentrations of 0.4–4.0%, without additional thickening agent. The microstructure and physical properties of the oleogels such as oil binding capacity, rheology, texture, thermal and oxidative stability were evaluated, using a variety of tools including confocal laser scanning microscopy, polarizing light microscopy, fourier transform-infrared spectroscopy and X-ray diffractometer. The adsorption and closely packing of CNF crystals on the surfaces of the oil droplets in emulsion decreased the clustering of droplets, and inhibited the oil droplets from destabilization during drying. This formed a more reticulated and denser but less anisotropic network, contributed to a β polymorph of the lipid crystallization. Thus the oil binding capacity and stability of oleogels were greatly enhanced, while stronger gelation strength, higher hardness, lower mobility and opaque appearance of the oleogels were observed. The oil loss of oleogels after processing at cooking temperature of 90 °C was remarkably declined, while the oxidative stability of the oleogels was also improved to a satisfactory level. In summary, these results contributed to a better understanding of the oleogelation in CNF-based oleogels, and benefited the use of healthy walnut oil to develop functional fat products with desired physical properties and oxidative stability.

1. Introduction

The extensive usage of saturated and hydrogenated fats has been reported to cause adverse health effects, such as increasing the risk of cardiovascular diseases, type II diabete and metabolic syndrome (McClements, 2020). The replacement of these fats by vegetable oil without seriously changing or weakening their processability in foods encourages researches to study oleogel formulations (Pehlivanoglu et al., 2018). For the formation of an oleogel, the use of gelling or structuring agents (named as oleogelators) in the oil is essential to confer a solid-like structure, a three-dimensional network capable of retaining large quantities of liquid oil. At present, the direct technology for structuring vegetable oleogels is becoming more mature, using low molecular weight compounds (like fatty acids, fatty alcohols, monoacylglycerols, wax, and phytosterol mixture) or large molecular ethylcellulose (EC) as the oleogelator (Davidovich-Pinhas, 2019; Meng, Qi, Guo, Wang, & Liu, 2018a). However, to a large extent, for the purpose of improving processability and seeking better texture and mouthfeel of

* Corresponding author.
** Corresponding author.
*** Corresponding author. College of Food Science and Technology, Yunnan Agricultural University, 425 Fengyuan Road, Kunming, 650201, Yunnan, People's Republic of China.
E-mail addresses: luojia@xtbg.ac.cn (J. Luo), shengjun_ynau@163.com (J. Sheng), tianyang1208@163.com (Y. Tian).
[1] Contributed equally to this paper.

https://doi.org/10.1016/j.foodhyd.2023.108849
Received 6 January 2023; Received in revised form 21 April 2023; Accepted 2 May 2023
Available online 2 May 2023

the resultant oleogel product (Pehlivanoglu et al., 2018), novel gelators from natural resources are still attracting more and more attentions (Phoon & Henry, 2020). Particularly, the direct oleogelation technology requires intensive heating to ensure the glass transition transformation of oleogelators (temperature of >80–90 °C for low molecular weight compounds and >140 °C for EC) and facilitate their dispersion in oil solvent (Davidovich-Pinhas, Gravelle, Barbut, & Marangoni, 2015). But it is not friendly for some heat or air-sensitive oils like walnut oil. Thus, it is meaningful to employ edible food-grade polymers such as polysaccharides to fabricate novel vegetable oil products rich in unsaturated fatty acids. The recommended polysaccharides should have unique interface characteristics and are renewable resources. Except for oleophilic EC and methylcellulose (MC), several cellulose derivatives with some enhanced hydrophilicity, like microcrystalline cellulose, carboxymethyl cellulose (CMC), α-cellulose, hydroxyethyl cellulose, hydroxyl propyl cellulose, hydroxyl propyl methyl cellulose (HPMC), regenerated cellulose (RC), and several natural fibers have also been used to produce oleogels (Pernetti, van Malssen, Flöter, & Bot, 2007).

The emulsion-templated approach is a promising method for most food-approved polymers that are inherently hydrophilic in nature, and thus cannot be dispersed easily in oil to achieve the structure formation required for gelation (Jiang et al., 2018). The method prepares an oil--*in*-water emulsion, followed by the removal of water to obtain dried products as physically-trapped oil through several drying methods (Jiang et al., 2018). The reported cases could be vegetable oleogels prepared by hydroxyl propyl methyl cellulose (HPMC) and methyl cellulose (MC), two cellulose ethers (Espert, Salvador, & Sanz, 2020; Meng, Qi, Guo, Wang, & Liu, 2018b), or by HPMC plus thickening agents such as carboxymethyl cellulose (CMC), xanthan gum, sodium alginate, arabic gum, guar gum, flaxseed gum or locust bean gum (Meng et al., 2018a; 2018c). A water-soluble polymer, regenerated cellulose (RC), derived from chemical treatment of microcrystalline cellulose, could also be used as co-oleogelator with carboxylmethyl cellulose (CMC), and successfully structures sunflower oil after emulsion-templated method and freeze-drying (Jiang et al., 2018). Recently, Phoon & Henry reported that edible oleogels and oleogel-based products such as breakfast spread and shortening-replacer could be produced using only natural food fibres (two insoluble fibres, citrus fibre and nata de coco fibre) *via* non-thermal emulsion-templated method and freeze-drying (Phoon & Henry, 2020).

Nanocelluloses, including cellulose nanocrystals (CNCs), cellulose nanofibers (CNFs), and bacterial cellulose (BC), with at least one dimension in the nanoscale range, are one of the most representative structuring materials. They are abundant and renewable resources, and have extraordinary mechanical properties as fiber materials (Perumal, Nambiar, Moses, & Anandharamakrishnan, 2022). Nanocelluloses have many other fascinating properties including large specific surface area, good modifiability, biocompatibility and biodegradability. Therefore, they have many application prospects, for instance, the dispersant for Pickering emulsion (Chu, Sun, Wu, & Xiao, 2020). More appealing aspects of those nanocelluloses include their anisotropic fiber structure, which favors stabilizing oil/water (O/W) interfaces at very low cellulose loading level. Semi-flexible CNF has been successfully used to stabilize many oil-*in*-water Pickering emulsions (Lu, Li, Ge, Xie, & Wu, 2021). This type of nanocellulose has been known to form stable gels (mainly hydrophilous till now) without the aid of temperature or cations (Mendoza, Batchelor, Tabor, & Garnier, 2018). Edible oleofilms were fabricated by casting beeswax-in-water Pickering emulsions stabilized by bacterial cellulose nanofibrils (BCNFs, a type of nanocelluloses) and carboxymethyl chitosan (CCS) (BC/CCS). The mechanical properties of the oleofilms were significantly improved by enhancing the ratio of BC/CCS (Li et al., 2020). However, relative reports are still limited. In addition, the surface properties of nanocellulose could be easily tuned by chemical modifications, which opens more possibilities of regulating oleogel morphology and final properties.

Walnut oil is rich in monounsaturated and polyunsaturated fatty acids such as oleic acid (12.4%–18.7%), linoleic acid (63.0%–68.9%) and α-linolenic acids (8.31%–8.68%). It exhibits multiple health benefits including the reduction of total plasma cholesterol and low density-lipoprotein cholesterol, and thus helps in decreasing the risk of coronary heart disease (Kalogiouri et al., 2021; Rebufa, Artaud, & Dreau, 2022; Sun et al., 2022; Yu et al., 2022). Because of these unsaturated components, this healthy edible oil is easily to be oxidized.

In this study, walnut oil emulsions were prepared with CNF as the sole emulsifier, and without any other thickening agent. The well-dispersed emulsions were then freeze-dried, and finally sheared to prepare oleogels. The objective of this study was to analyze the effects of CNF concentration on the formation, structure and properties of the constructed oleogels. To be more specific, the effects of CNF concentration on the microscopic morphology, molecular and crystalline structure, oil binding capacity, rheological characteristics, texture properties, thermal stability and oxidative stability of the formed oleogels were investigated. The mechanisms underlying the function of CNF during the formation of oleogels were discussed. This work provides the essential and useful information on the molecular interactions responsible for the formation of CNF-based oleogels and property control of the edible oleogels constructed with nanocelluloses. We also hope it to be a good start for the study of high-value vegetable oleogels structured by green and diversified cellulose factors in future.

2. Materials and methods

2.1. Materials

Cellulose nanofiber/nanocellulose (CNFs, particle diameter of 5–10 nm, 0.8–2.0 μm long, 1.80 mmol/g carboxyl groups) at 1.0% (w/w) aqueous solution was commercially available from Woodelfbio biological technology co., Ltd (Tianjing, China). Ammonium thiocyanate and ferrous chloride were purchased from Shanghai Macklin Biochemical Co., Ltd (Shanghai, China). Cumene hydroperoxide, 1,1,3,3-tetramethoxypropane and 2-thio-barbituric acid-reactive substances (TBARS) were purchased from Aladdin BioChem Technology Co., Ltd (Shanghai, China). Nile red and Calcofluor white were purchased from Sigma-Aldrich. Virgin walnut oil was purchased from the local supermarket, which was produced by Yunnan Dianxue Grain and Oil Co., Ltd. (batch number: 01WT20220671), using hot pressing method without further refinery. It has a water and volatile content of 0.02%, an acid value of 2.1%, and a peroxide value (POV) of 0.092%. High-purity water with the conductivity of 12–18.2 mΩ cm was provided by a laboratory water purifier (FST-JY-80). All other chemicals used were of analytical grade.

2.2. Preparation of emulsion-templated oleogels

Emulsions and the corresponding oleogels were prepared based on the procedures as described by Patel et al. (Patel, Rodriguez, Lesaffer, & Dewettinck, 2014) with minor modifications. Briefly, CNF solutions (16 mL) were prepared by diluting 1.6–16 mL aqueous CNF solution (1.0%) with distilled water and homogenized with a high-speed homogenizer (HR-500, Huxi, China) at 1,000 rpm for 2 min. Walnut oil (4.0 mL) was dispersed in CNF solution to prepare an emulsion with water as the continuous phase using a high speed dispersing machine (Ultraturrax, IKA, Germany) at 13,000 rpm for 3 min. The prepared O/W emulsion was subsequently freeze-dried by a Vacuum Freeze Dryer (FD-1, Biocool, Beijing, China) over 48 h (condenser: < −50 °C, vacuum: < 20.0 Pa) to produce soft solid, which was then smashed and sheared (40 s) using a grinder and a high speed dispersing machine (10,000 rpm) to obtain oleogels with different CNF loadings (0.4–4.0% w/v, relative to the volume of walnut oil).

2.3. Morphology and microstructure observation of emulsions and oleogels

Optical microscopy of the emulsions was conducted using a microscope (Olympus CX43RF, Tokyo, Japan) with a digital camera (Nikon, Japan). The emulsion type was determined by drop test, whereby a droplet of the formed emulsion was added to water or oil. If the droplet could be dispersed in water then the emulsion type was O/W, and vice versa if the droplet was well dispersed in oil. Additionally, confocal laser scanning microscopy (CLSM, ZEISS LSM700, Germany) was used to further confirm the emulsion type. The oil phase and CNF was labeled with fluorescent Nile red and Calcofluor white, respectively. An aliquot (1 mL) emulsion was stained with 20 μL of a staining solution containing 0.1 wt% Nile red and 0.01 wt% Calcofluor white, and then incubated in dark for 2 h. After staining, the samples were dropped on a micro-scope slide, covered with a coverslip and analyzed on the CLSM system using a 40 × objective lens at an excitation wavelength of 405 nm for Calcofluor white and 488 nm for Nile red, respectively.

Oleogel morphology was observed with polarized light microscopy (PLM) (Nikon E600POL, Nikon Optical Co., Ltd., Tokyo, Japan), with images under bright-field captured using a digital camera. Oleogels at different CNF concentrations were poured on a clean preheated glass microscope slide and gently covered with a preheated glass coverslip. The samples were kept at 4 °C overnight before observation. The photomicrographs were taken with a 20 × objective lens. A number of images were acquired, each of which represented a typical field. The samples were analyzed at ambient temperature and each analysis was carried out in triplicates.

2.4. Critical gelling concentration of oleogels

The gelation state of the prepared oleogels was judged by critical gelling concentration. Briefly, around 0.5–1.0 g of samples at different CNF concentration were filled in 2 mL plastic centrifuge vials, and then the vials were inverted to observe the fluidity of samples. The initial interval of CNF concentration was set to 1.0% (namely, concentration of 1.0%, 2.0% and 3.0%) for the facility of determining the approximate gelation range of samples. Then, it was gradually reduced to an interval of 0.1%. The sample with the lowest CNF concentration that did not flow was considered to be the critical gelling concentration.

2.5. Oil binding capacity of oleogels

The oil binding capacity of oleogels was measured using centrifuge method (Meng, Qi, Guo, Wang, & Liu, 2018c). Briefly, a precise oleogel amount of 1.0000 g (m_1) was weighed in a 1.5 mL plastic centrifuge vial and was centrifuged at 10,000 rpm for 15 min. The supernatant as released liquid oil was removed completely. Then, the centrifuge vial was weighed again (m_2). Oil loss values were calculated by employing Eq. (1), where m_1 was the mass of initial sample and m_2 was the sample mass after draining all unstructured oil.

$$\text{Oil loss} = (m_1 - m_2) \ / \ m_1 \times 100\% \quad (1)$$

The oil binding capacity of oleogels was determined as:

$$\text{Oil binding capacity} = (1 - \text{Oil loss}) \times 100\% \quad (2)$$

2.6. Rheological measurements

The rheological measurements were performed with a rotational rheometer (MCR 302, Anton Paar, Graz, Austria) using a parallel-plate measuring system (PP25). The gap between two plates was set to 1.0 mm. Amplitude sweeps, frequency sweeps and temperature sweeps were carried out. For the CNF-based oleogel samples, amplitude sweeps (strain: 0.001%~100%, frequency = 1 Hz) and frequency sweeps (frequency = 0.1–100 Hz, strain: 0.02%) were performed to study the viscoelastic properties of oleogels. The limit of the linear viscoelastic region (LVR) was calculated in term of ±5% deviation for storage modulus around the plateau value. All the above measurements were carried out at 25 °C. Temperature sweeps (Temperature variation: 20 °C–90 °C at a rate of 5 °C/min, frequency = 1 Hz) were conducted within strain at 0.02%.

2.7. X-ray diffraction (XRD)

Structural properties of CNF powders and oleogel samples were studied using an X-ray diffractometer (Ultima IV, Rigaku, Japan). The X-ray source was a copper X-ray tube (CuKα1; $\lambda = 1.5406$ Å) operating at 40 kV and 40 mA. Diffraction patterns were acquired at diffraction angles (2θ) of 5–60° at a scanning rate of 4°/min at room temperature. The data were collected and analyzed using the software MDI Jade 6 (Materials Data Inc., Livermore, USA). A well-known Scherrer equation (Eq. (3)) was introduced to roughly estimate the crystalline dimension (D, Å) of oleogel particles without further instrumental calibration:

$$D = K \times \lambda \ / \ (B \times \cos\theta) \quad (3)$$

Where K was the Scherrer constant speculated as 0.89, B was the full width at half maxima of the crystalline peak used for calculation.

In oleochemistry, the short spacing between crystalline planes was defined as the distance between parallel acyl groups of triacylglycerol molecules in structured oil systems, and thus reflected the mode for the subcell packing of lipid molecules in the systems, or was used to distinguish the polymorphic forms based on their X-ray diffraction patterns (Metin & Hartel, 2020). The short spacing (d, Å) in this study was calculated by the following equation:

$$d = n \times \lambda \ / \ (2 \sin\theta) \quad (4)$$

Where n could be 1, 2, 3, 4 or other multiples.

2.8. Fourier transform-infrared spectroscopy (FTIR)

The FTIR spectra of CNF powders and oleogel samples were recorded using an FTIR spectrophotometer (Nicolet IS10, Thermo Nicolet Ltd., USA). The CNF powder was grounded with KBr in an agate mortar and pressed into a pellet according to a standard procedure, while the acquisition of the FTIR spectrum of CNF followed the transmission pattern. The spectra of pure oil and oleogel samples were collected with the auxiliary of an attenuated total reflectance (ATR) sampling accessory. All spectra were recorded within the wavenumber range from 4000 to 400 cm^{-1} at a resolution level of 4 cm^{-1} and over 32 scans.

2.9. Texture analysis

Oleogel samples after shear were used in texture measurements. The samples were placed in cylindrical containers (30 mm internal diameter × 15 mm height) and equilibrated for 1 day at room temperature. Penetration test was performed using a FTC/TMS-Touch Texture Analyzer (Food Technology Corporation, USA) with a 50 N load cell. The samples were penetrated with a cylindrical probe (10 mm diameter) with a 0.05 N trigger force. Penetration was set to a depth of 6 mm at a rate of 1 mm/s. Force-time profiles were recorded for calculating the maximum force and the area under the curve (AUC). The reported values were average of three repetitions.

2.10. Assessment of thermal stability of oleogels

Thermal stability of the oleogels was measured as the method described by Phoon & Henry (Phoon & Henry, 2020) with some modifications. Briefly, 2.0 g of each oleogel sample was placed in a 15 mL plastic centrifuge tube, and was incubated for 30 min in a water bath of 30, 50, 70 and 90 °C, respectively. The morphological differences of the

oleogel samples were observed immediately under an optical microscope (Olympus CX43, Tokyo, Japan). Then, the tube was centrifuged at 10,000 rpm for 15 min at room temperature. After the removal of supernatant completely, the centrifuge tube was weighted. The values of oil loss were calculated as described above in Section 2.5.

2.11. Oxidative stability of oleogels

The oxidative stabilities of walnut oil and CNF-based oleogels were assessed by the accelerated oxidation test. Around 2 g of walnut oil and oleogel samples were equally added into 2 mL glass tubes, respectively. Then the tubes were sealed and stored in the dark at 37 °C for 15 days. Lipid oxidation was determined using POV and thiobarbituric acid reactive substances (TBARS) values (Pan et al., 2021). Briefly, POV was determined by lipid hydroperoxide using a ferric thiocyanate method. The hydroperoxide concentration was determined using a standard curve made from cumene hydroperoxide. TBARS were determined by mixing 0.5 g oleogels or 0.3 mL walnut oil with an aqueous solution containing 15 wt% trichloroacetic acid, 0.375 wt% thiobarbituric acid, and 2 wt% HCl. The mixtures were heated in a water bath of 90 °C for 20 min, cooled to room temperature and centrifuged at 3,600 g for 15 min. The absorbance of each supernatant was measured at 532 nm. The TBARS concentration was determined from a standard curve prepared with 1,1,3,3-tetraethoxypropane. All the measurements were carried out in triplicate.

2.12. Statistical analysis

Statistical analysis was carried out using Origin 8 and Sigma Plot 12.5. All the measurement data were presented as means with standard deviation and differences were considered significant at 5% ($P < 0.05$).

3. Results and discussions

3.1. Emulsions morphology

Stable dispersion is a prerequisite for all envisioned nanocellulose products to meet quality control specifications (Foster et al., 2018; Shao et al., 2020). As shown in Fig. 1a, the walnut oil emulsions (O/W) with CNF concentration from 0.2 to 2.0% were prepared firstly. The fresh emulsions dispersed well at all the studied CNF loadings, and no visible phase separation was observed for at least 30 min (Figs. 1a at 0.5 h). This confirms that CNF can stabilize oil/water interfaces efficiently due to their amphiphilic surface characteristics originating from the

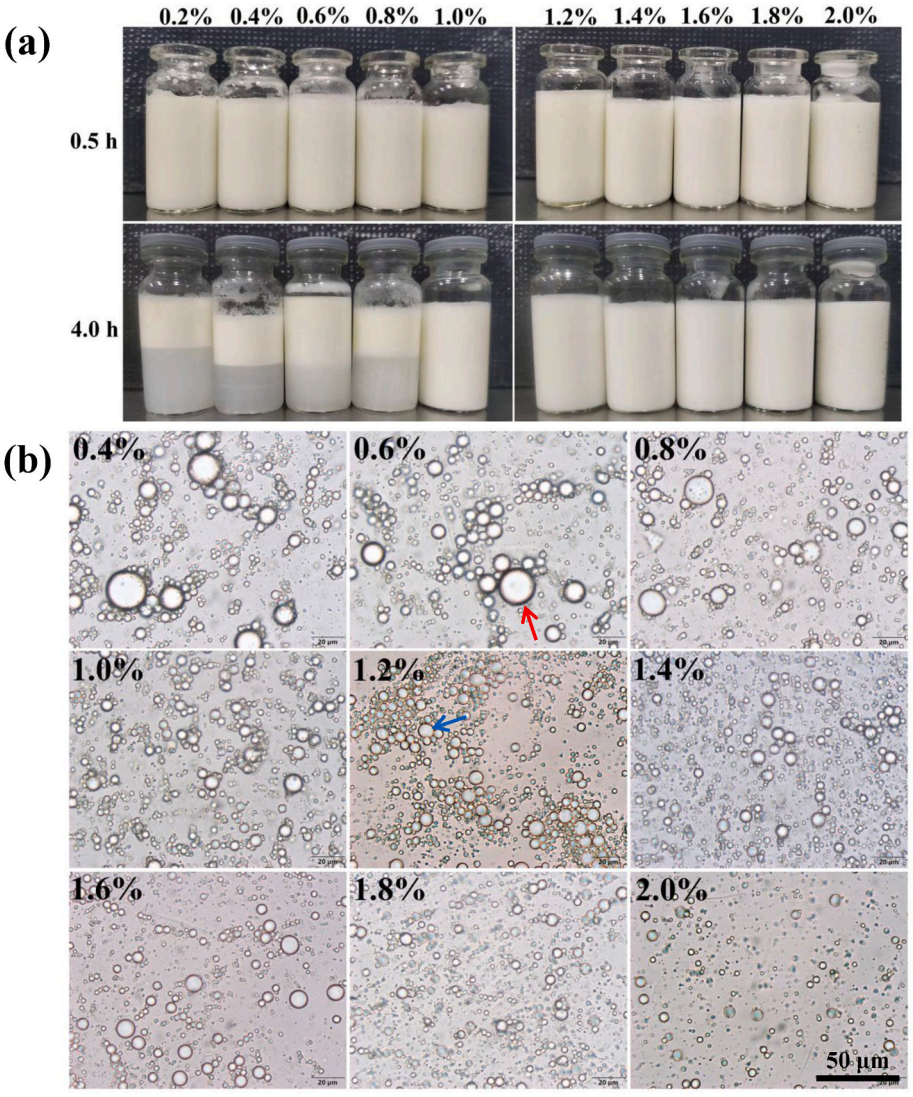

Fig. 1. The appearance (a) and optical micrographs (b) of the walnut oil-*in*-water emulsions stabilized by CNF with various concentrations (relative to oil phase). The scale bar is 20 μm. The red arrow indicates "planet-satellite-like cluster structure", blue arrow indicates "grape cluster-like cluster structure".

hydrophobic face and hydrophilic edge of cellulose chains (Fujisawa, Togawa, & Kuroda, 2017). However, the walnut oil emulsion was a typical thermodynamic unstable system. After standing for 4 h at room temperature, the emulsions with CNF concentration of 0.1–0.8% remarkably creamed (Figs. 1a and 4 h), which was not observed when the concentration of CNF was higher than 1.0%. Semi-flexible fibers with certain length are able to be adsorbed on the surface area of neighboring oil droplets and provide strong steric hindrance for stabilizing emulsions (Lu et al., 2019). Meanwhile, the intermolecular interaction between CNF chains was not strong enough to induce remarkable gelatinization of CNF factors, like the situation of bacterial cellulose with very long length of ~20 μm and super-flexibility (Lu et al., 2021). This point eliminated the hindrance for breaking-down bulk oil, and facilitated the migration of CNF particles towards the O/W interface. However, when the concentration of CNF was below 1.0%, it was not sufficient to fully emulsify all O/W interfaces. Significant number of droplets needed to share CNF particles with other droplets for the purpose of maintaining emulsion stability, which increased collision between droplets, and resulted in local agglomeration or partial flocculation, just as the morphology of emulsions after 4 h standing (Fig. 1a).

The emulsions prepared at varying CNF concentrations were evaluated for morphology of oil droplets using an Olympus CX43 microscope under bright field. Typical cluster structure with broad or even multimodal size distribution was seen in walnut oil-*in*-water emulsions with CNF concentration of 0.4–1.8% (Fig. 1b). This was possibly ascribed to the complex constitution in walnut oil: short-chain components of walnut oil formed small droplets, while those long-chain ones were responsible for larger droplets during emulsification (Ostertag, Weiss, & McClements, 2012). The formation of droplet cluster structure was regarded as the results of depletion flocculation mechanism, which dominated the stabilized emulsion structured by CNF factors (Lu et al., 2021). Namely, the exclusion of CNFs from the confined region surrounding each oil droplet produced a concentration gradient between the region with high CNF loadings and the 'depletion zone' surrounding droplets, which attracted neighboring droplets approaching *via* entropy-driven pattern. However, with the increase of CNF loading, the morphology of droplet clusters gradually evolved from the planet-satellite-like structure (CNF loading of 0.4–0.8%) to the grape cluster-like one (CNF loading of 1.0–1.4%) (Lu et al., 2019), and finally disintegrated (CNF loading of 2.0%) (Fig. 1b). The droplet size of emulsions was significantly reduced with the increase of CNF loading, which also had great influence on the stability and flowability of emulsions. It possibly demonstrated that the development of percolation network with the increase of CNF loading provided increasing effectiveness in steric hindrance and coverage protection, which further enhanced the ability for inhibiting the coalescence of emulsion droplet (Lu et al., 2021).

The oil-water interface is considered to be the critical area for emulsion stabilization, as it is the main contact region between walnut oil and amphiphilic CNF. The confocal laser scanning microscopy (CLSM) image in Fig. 2 depicted an emulsion microstructure attained in the sample preparation, which exemplifies a random close packing of the dispersed droplets surrounded by continuous water phase and stabilized by CNF. Fig. 2a showed the oil phase, labeled in red, surrounded by an unlabeled aqueous phase, confirming that the emulsion was of the O/W type. Fig. 2b showed the cellulose, labeled in fluorescent blue (Calcofluor white stains CNF), and the isolated drops with fluorescent surfaces, confirming that the surface of oil droplets were completely or largely covered with adsorbed cellulose, while unadsorbed cellulose was also observed in the continuous phase (Fig. 2c) (Shen, Guo, Wu, Zhang, & Abid, 2016). It again verified the stabilization role of CNF when it was adsorbed at the O/W interface. In contrast, walnut oleogel structured by 4% candelilla wax required additional 2% potato starch to steady the oil-water interface (Wang et al., 2022).

3.2. Critical gelling concentration (CGC) and oil binding capacity (OBC) of CNF-based oleogels

The emulsion samples prepared at different CNF concentrations were freeze-dried to remove moisture, which yielded oily solid. It could be seen in Fig. 3a that the highly structured emulsions were stable enough during drying process without visible coalescence of oil droplets. As drying progressed, the intermolecular interactions between CNF molecules absorbed on O/W interfaces were enhanced, which might result in more densely packing of CNF particles on O/W interfaces, as well as the thickened droplet surface layer. This protected oil droplets from coalescence, and provided white, porous and fluffy cotton-like appearance for the samples with CNF concentrations of 1.2–4.0%. In other words, the density of CNF aggregation significantly affected the appearance of oleogels, which showed lower transparency when it was with larger and denser aggregation (Fig. 3b). After shearing, the resulting oleogels contains >97 wt% walnut oil (analyzed by Soxhlet extraction method), and were thus good templates for obtaining dried oil products.

The minimum concentration of gelators required for the transformation of liquid oil into a gel structure is called the critical gelling concentration (CGC), which reflected the gelation ability of a gelator. The CGC value of CNF-based oleogel was in the range of 0.3–0.4% (Fig. 3b). When CNF concentration was below 0.4%, remarkable oil leak was detected after shearing of the dried soft solid, which indicated that the gelling network structured by less than 0.4% CNF could not effectively trap liquid oil. Thus the resultant product could not be regarded as

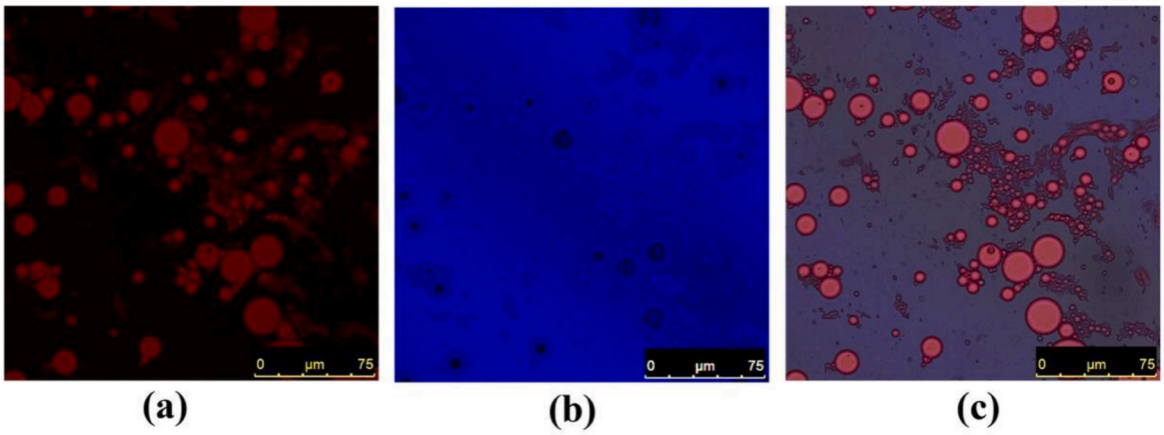

Fig. 2. Confocal laser scanning microscopy image of the walnut oil-*in*-water emulsion stabilized by 1.2% CNF concentration (relative to oil phase), stained by Nile red dye (a), Calcofluor white (b), and both Nile red and Calcofluor white (c), respectively. The scale bar is 75 μm.

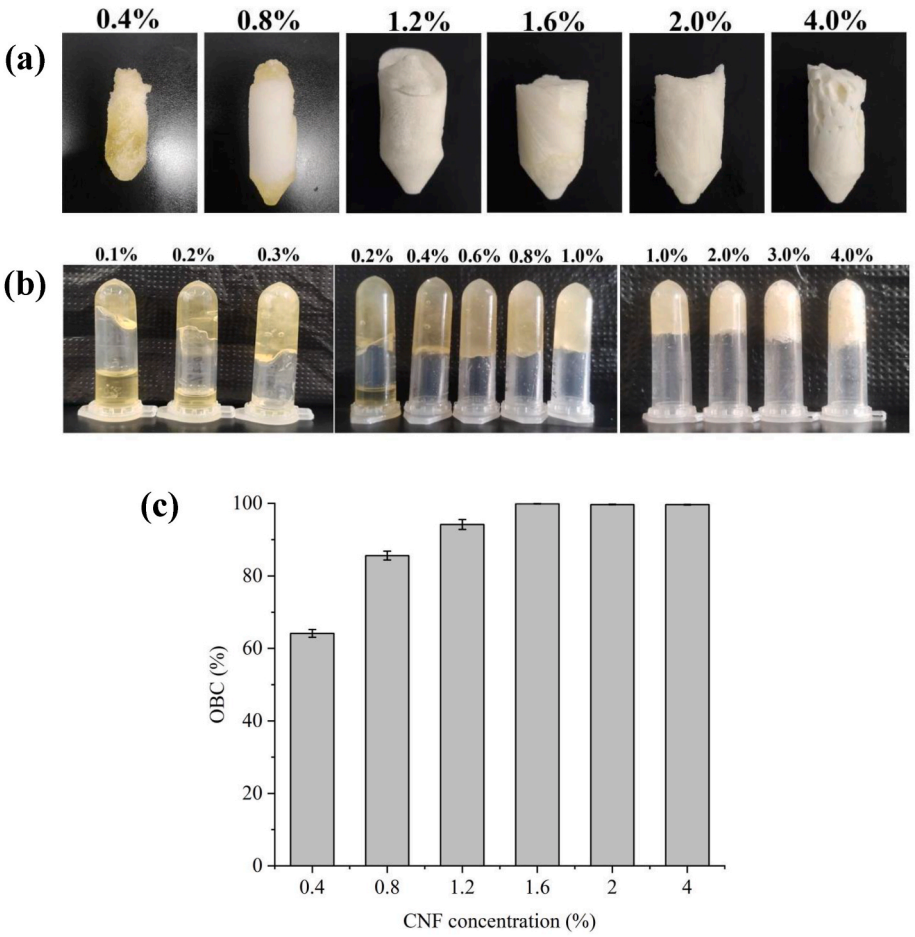

Fig. 3. Macrophotographs of the walnut oleogels with various CNF concentrations. (a), Surface appearance of oleogels (before sheared); (b), surface appearance of oleogels (after sheared); (c), the oil binding capacity of the oleogels.

the true gel system. But this phenomenon was not happened for oleogel samples with CNF concentration of higher than 0.4%. Therefore, in the following sections, oleogels with CNF concentration of higher than 0.4% were allowed to be used in structure characterization and property analysis.

The oil binding capacity (OBC) was a sign of the interactions between liquid oil and the gelator molecules (Blake, Co, & Marangoni, 2014). In Fig. 3c, the OBC values of the CNF-based oleogels were all above 60%. And as the increase of CNF concentration from 0.4% to 1.6%, the OBC values of oleogels increased to around 97%, which indicated the significant effect of CNF loading on OBC. These values were comparable to the OBC of monoacylglycerol (MAG)-based oleogel with cold pressed walnut (around 88%) (Sun et al., 2022) and the value of oleogel structured by Candelilla wax and potato starch (around 89.1%) (Wang et al., 2022).

3.3. Rheological properties of oleogels

Rheological properties of oleogels were determined at CNF concentrations of 0.4–4.0% (Fig. 4). In amplitude sweeps at frequency of 1 Hz (Fig. 4a), the storage modulus (G') of all tested oleogel samples remained nearly constant as the strain increased from 0.001% to 0.06%, which could be defined as the linear viscoelastic region (LVR) of CNF-based oleogels. In this LVR, storage modulus (G') > loss modulus (G"), which suggested the strong gelation strength and representative solid-like behaviors of the oleogels. With the further increase of strain level, the G' of CNF-based oleogels showed a regular decreasing trend, while the G" of CNF-based oleogels showed a slight increasing soon followed by an obvious decreasing. Similar to the trend reported in oleogels structured by other polysaccharide factors (Meng et al., 2018a; 2018c), a crossover point of G' and G" curves (namely yield point) was observed at the strain of 0.74–2.66%, demonstrating liquid behaviors of oleogels at higher strain values. The gelation strength (G') of oleogels was gradually enhanced with the increase of CNF loadings, which were $3.7 \pm 0.32 \times 10^4$ and $4.8 \pm 0.09 \times 10^5$ Pa at strain level of 0.02% for CNF loadings of 0.4% and 4.0%, respectively. The G' of CNF-based oleogels were comparable to 12% β-sitosterol/γ-oryzanol-based walnut oleogels ($\sim 9 \times 10^5$ Pa, Xu, Sun, Zhang, & Wang, 2020) and MAG-based walnut oleogels ($\sim 4 \times 10^5$ Pa, Sun et al., 2022).

In Fig. 4b, frequency sweeps of oleogels were conducted at strain level of 0.02%. The G' values of the oleogels were larger than those of G" at all frequencies. Both G' and G" of all oleogels increased as a result of the increase in CNF concentration, which exhibited weak frequency dependence. Higher G' and G" moduli were obviously obtained in 4.0% CNF based oleogel than those at lower CNF concentrations. The G' values of 2% CNF-based oleogels were 4 times bigger than those of 2% regenerated cellulose (RC) and 1.4% CMC-based oleogels ($\sim 2.2 \times 10^4$ Pa, Jiang et al., 2018). Temperature sweeps were conducted to measure the thermal sensitivity of oleogels during the heating stage (Fig. 4c). The G' and G" moduli of CNF-based walnut oleogels were nearly unchanged with the increase of temperature, indicating a high thermal stability of the obtained oleogels.

3.4. Texture measurements

The mechanical properties of the final oleogels were determined by

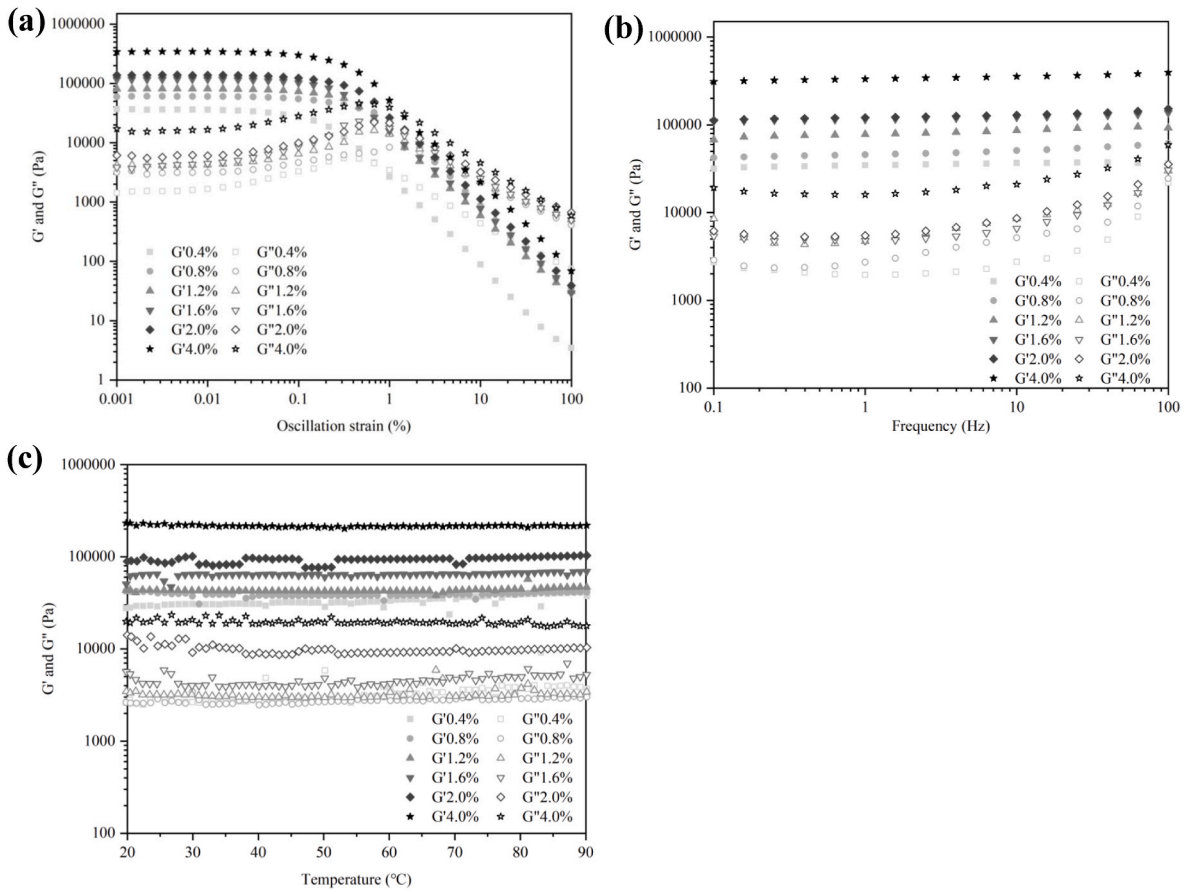

Fig. 4. Amplitude sweep (a), frequency sweep (b) and temperature sweep (c) curves for the walnut oleogels with different CNF concentrations.

penetration tests on a Texture Analyzer. The texture curves of the oleogels obtained from 0.4% to 4.0% CNF emulsions were shown in Fig. 5. Similar to previous literature (Espert et al., 2020), the force increased linearly as the function of penetration time, while no sudden rupture peak or force drop was observed before the penetration reached the appointed depth of 6 mm. It meant that neither evident deformation nor serious destruction of gel structure occurred during the penetration test. The force-time profiles showed the typical characteristic of a compact gel structure. The hardness of oleogels and the work expended in penetration were recorded as the values of maximum force (Fig. 5B) and the area under the curve (AUC, Fig. 5C), respectively. As the penetration was advanced at a constant rate of 1 mm/s, the value of AUC was just the value of the work expended in penetration. For 0.4% and 0.8% CNF-based oleogel, low hardness and AUC values were detected, which was 0.17–0.18 N and 0.65–0.88 N s, respectively. As the concentration of CNF was increased to 4.0%, the hardness value significantly increased to 9.88 N (Fig. 5B), accompanying by the rise of AUC to 34.41 N s. The hardness and AUC of 4% CNF-based oleogel were 10.2 and 8.1 times of the values for 2% CNF-based oleogel, respectively. Higher AUC value meant that it required more work to overcome the resistance from oleogel itself before the penetration destroyed the integrity of the inner gelled structure of oleogel and reached the appointed depth. This was also described by a commonly known term of gel consistency in some previous studies (Espert et al., 2020). In other words, the increase of CNF loading remarkably improved the hardness and consistency of the oleogels.

The hardness and AUC values of CNF-based walnut oleogels in this study were lower than the values of sunflower oleogels fabricated by MC or HPMC with similar gelator concentrations in a previous study (Espert et al., 2020). In that study, 0.89% MC or HPMC based oleogels gave maximum force of 2.18–2.52 N and AUC of 8.21–8.87 N s, while 1.77% MC or HPMC based oleogels gave maximum force of 6.61–6.99 N and AUC of 20.23–23.47 N s.

3.5. Thermal properties of oleogels

Oil loss of oleogel at higher temperature reflected the thermal sensitivity of oleogel structure (Phoon & Henry, 2020). Processing of oleogels at much higher temperature possibly resulted in the damage or even collapse of oleogel structure, and destroyed the capacity of gelation network for holding or trapping liquid oil. Severely structure collapse and apparently melting of the oleogels were observed at all tested temperatures for the sample structured by the lowest CNF concentration (0.4%) (Fig. 6a), which indicated the lowest thermal stability. For the sample containing more CNF (0.8%), the oleogels stayed basically stable till 70 °C, while slightly structure collapse and oil leaked-out were observed after heating at 90 °C. The oleogels with high CNF concentration (1.6%, 2.0% and 4.0%) were the most thermally stable, without any structure collapse and oil oozing from the structure even at 90 °C. The apparent melting behavior of these oleogels was different with the data of natural citrus fiber (Phoon & Henry, 2020), which showed more unstable with comparable fiber concentration (1.5% or 2.0%) indicating the fiber type indeed influence the thermal properties of polysaccharide-based oleogels.

The oil losses of the oleogels after heating were weighted in Fig. 6b, which demonstrated that the CNF concentration from 0.4% to 1.6% have important effects on the thermal stability of the oleogels. At CNF concentration of 0.4%, the oil losses were more than 40% after heating for 30 min at all tested temperatures of 30–90 °C, indicating the serious instability of the sample during heating process. As the increase of CNF concentration from 0.8% to 1.6%, the oil losses of these oleogels decreased significantly, while much higher loss was detected at higher

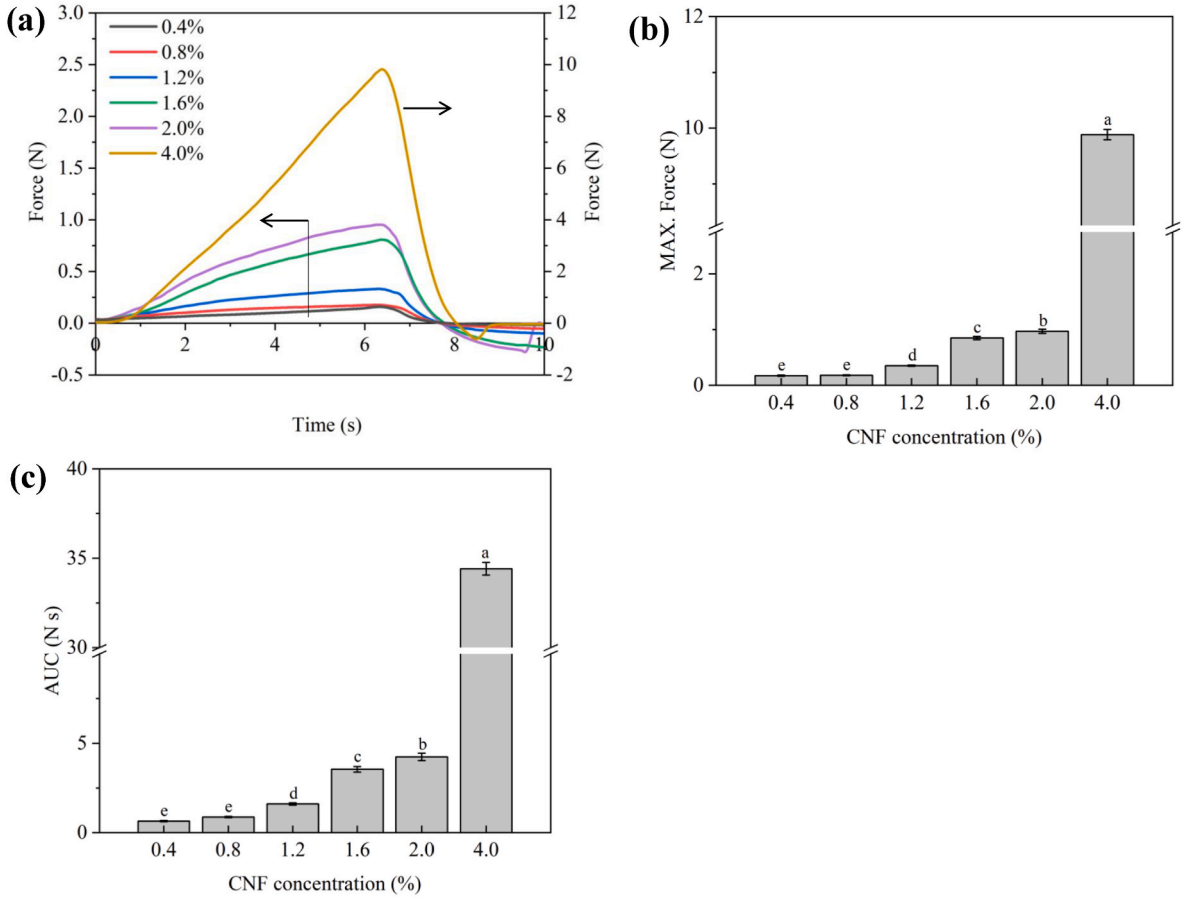

Fig. 5. Force-time profiles (a), MAX. Force (b) and area under the curve (c) of the walnut oleogels with different CNF concentrations. For Fig. 5a, oleogels containing 0.4–2.0% CNF referred to the left vertical axis, while oleogels containing 4% CNF referred to right vertical axis. a-e: different letters indicate significant differences ($p < 0.05$).

heating temperature at the same CNF concentration. At CNF concentration of 0.8%, the oil loss rose from 25.1% to 43.7% with the temperature elevated from 30 to 90 °C, while it was from 8.8% to 20.7% for CNF concentration of 1.6%. However, when the CNF concentration was higher than 2.0%, the oil loss sharply declined, which was no more than about 3% even at heating temperature of 90 °C, and indicated the highly stability of the corresponding oleogels.

3.6. Molecular properties of oleogels

3.6.1. Morphology of CNF-based oleogels

The macroscopic properties of oleogels are closely related to their microstructure. In order to better explain the effect of the gelator concentration on the formation of oleogels, the internal structure of the samples was observed by optical microscrope and PLM (Fig. 7a, optical; Fig. 7b, PLM). The oleogel seemed to be an aggregate of CNF polymer strands with liquid oil trapped in them (Fig. 7a). The oil was well dispersed throughout the fibrous network in each oleogel sample, without flowing or leaking out. Compared with the images of the corresponding emulsions (Fig. 1), the strands were speculated to be CNFs adhered by the liquid oil. With CNFs in the bulk phase and at the interface, oil droplets bounded to CNF factor and were separated without coalescence, which formed viscoelastic layer during emulsion-forming process. Then, during the freeze-drying process, oil droplets were possible to be out of shape with the removal of continuous water phase but not fractured, while CNF-stabilized oil droplets aggregated to build a stable three-dimensional network structure inside the oleogel.

The effect of CNF concentration on the strand density and oleogel morphology was significant from the PLM images (Fig. 7b), which was in accordance with the appearance of oleogels in Fig. 3b. Obviously, a lower concentration of CNF was not sufficient for fully and closely entrapment of walnut oil due to few and diffuse strands. And possibly, the stabilization of oleogel structure in this situation depended more on the interactions between CNF chains and oil molecules, rather than the physical functions provided by the hard boundary wrapping oil droplets. However, when the gelator concentration was increased, the number of fibrous units increased in the oleogel, and thus, a more reticulated network was achieved. The internal structure of the system became more closely linked, leading to a stronger network. More hydrophobic segments of CNF were absorbed to the oil interface, which remarkably improved the oil binding capacity of the prepared oleogels. The large number of clew-like crystals would pile up on each other to form dense and interlaced aggregates at the interface of O/W emulsion precursor, which finally turned to a thicken and hard shells at the surface of the trapped oil droplets during freeze-drying to protect them from coalescence, and thus resulted in the higher hardness (Fig. 5) and lower mobility of the oleogels. The difference in network formation possibly expressed itself in the macroscopic properties of the oleogels, possibly similar to that happened for protein-based oleogels (Foegeding, Bowland, & Hardin, 1995). Namely, fibrillar aggregates at lower CNF loading leaded to a more fine-stranded network, providing the oleogel with more elastic and transparent characteristics, while it was changed to a coarse network with an opaque appearance of the oleogel due to the denser aggregation with a concentrated CNF system (Fig. 7b).

From the PLM images (Fig. 7b), it could also be deduced that the anisotropy of oleogel structure obviously decreased with the increase of CNF concentration, although more fibrous units were added. There was a reasonable explanation that the anisotropy trend of oleogel

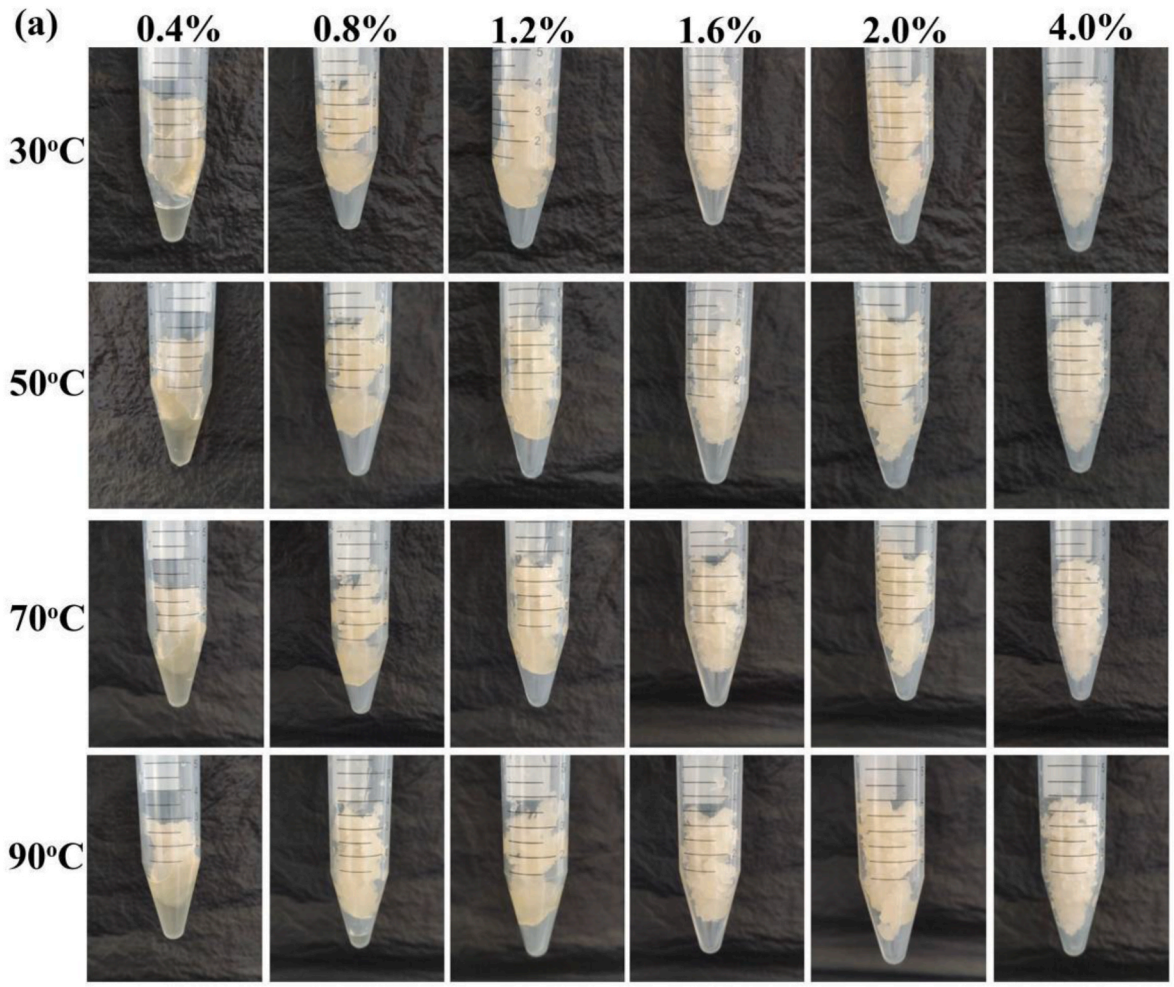

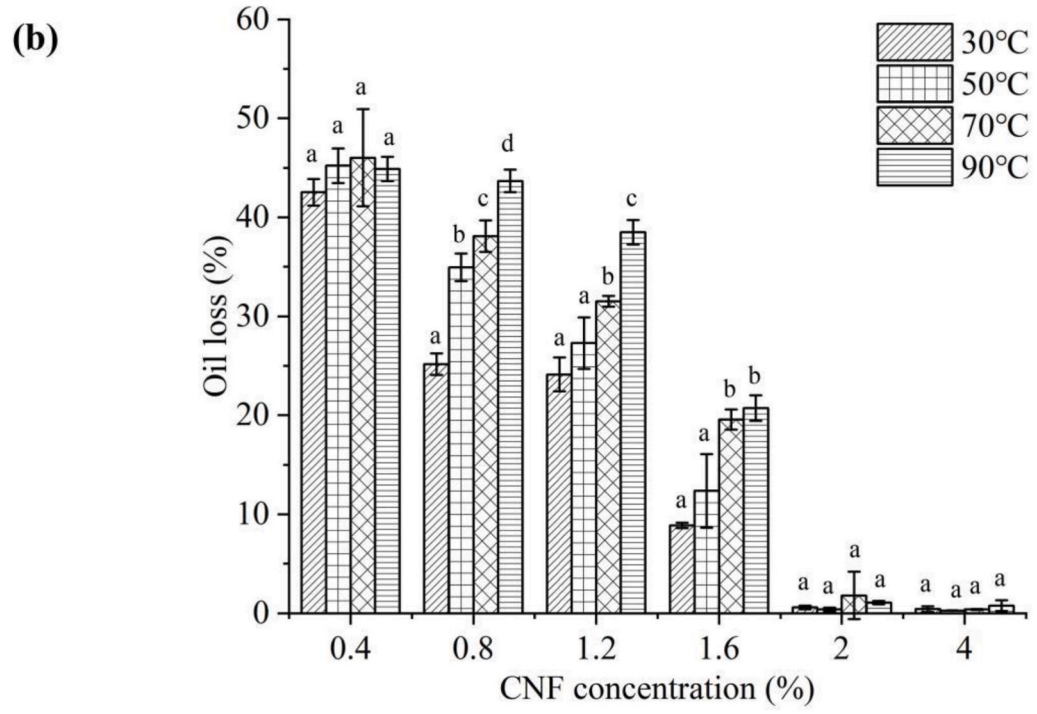

Fig. 6. Effect of CNF concentration on the thermal stability of walnut oleogels. The appearance (a) and oil loss (b) of oleogels contained 0.4%, 0.8%, 1.2%, 1.6%, 2.0% and 4.0% CNF. a-d: different letters indicate significant differences ($p < 0.05$).

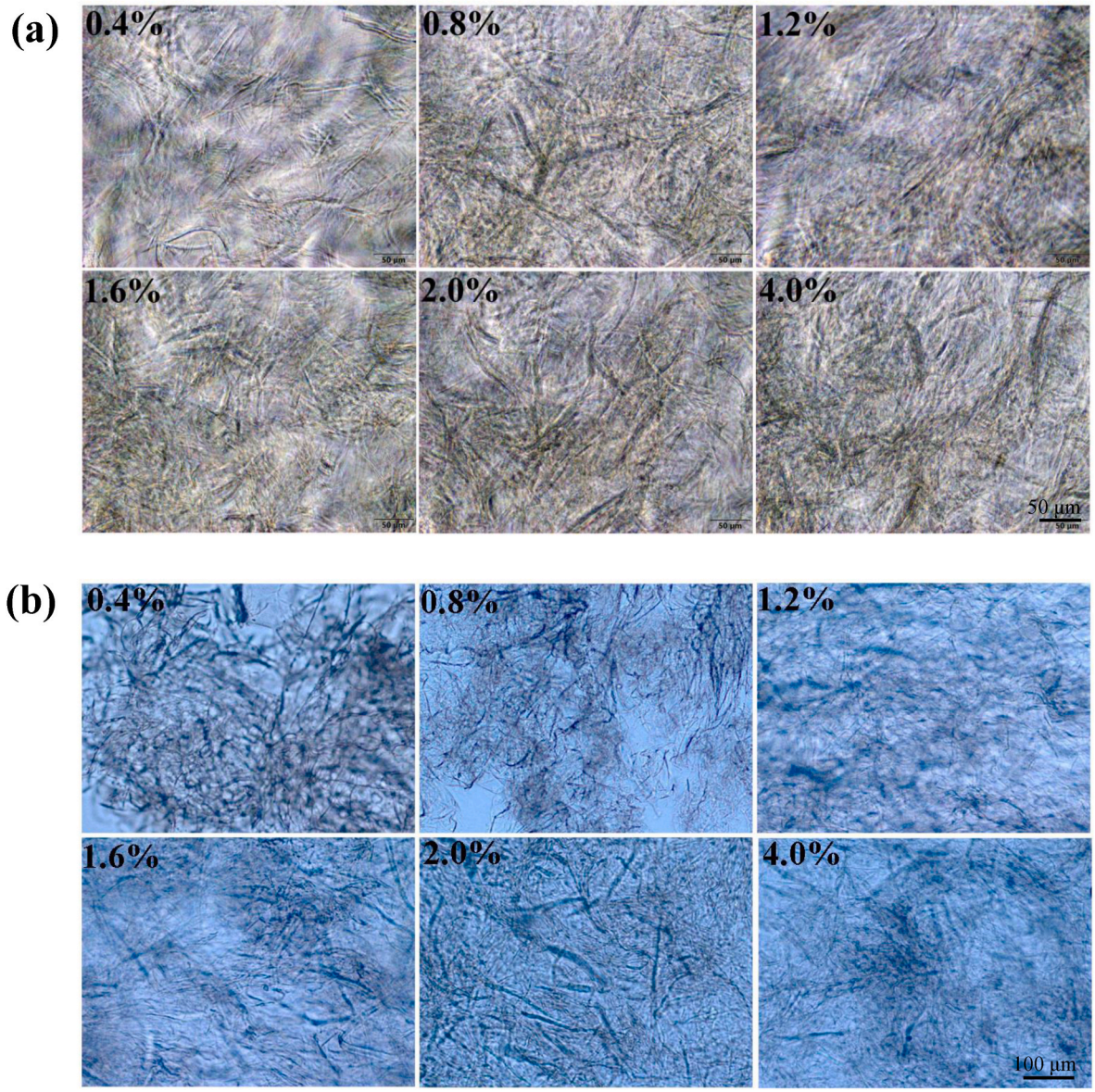

Fig. 7. Microstructural morphologies of the walnut oleogels contained 0.4%, 0.8%, 1.2%, 1.6%, 2.0% and 4.0% CNF by optical microscopy (a) and by polarized light microscopy (b).

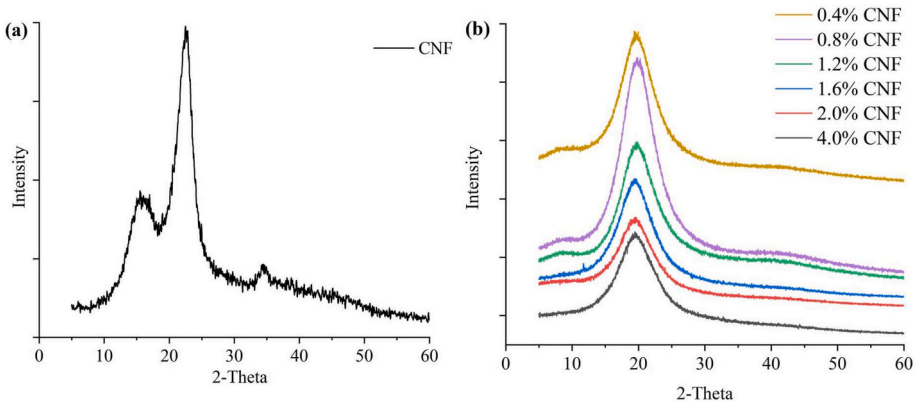

Fig. 8. X-ray diffraction patterns of the CNF powder and walnut oleogels contained 0.4%, 0.8%, 1.2%, 1.6%, 2.0% and 4.0% CNF.

microstructure possibly reflected the consequence resulting from the change droplet size and cluster structure of emulsion precursors containing different CNF concentration. It seemed that the large droplet size, multimodal size distribution and planet-satellite-like cluster structure of the emulsion with CNF loading of 0.4% might increase the possibility of coalescence or Ostwald ripening of droplets within droplet cluster during drying and crystallization process, which aggravated the anisotropy of the resulted gelation network. While for the emulsion with CNF loading of 2.0%, droplet cluster disintegrated with more isolated and uniformly distributed droplets, which was finally responsible for a more isotropic and firm gelation network of the resulted oleogel, and consequentially influenced the OBC, thermostability and other related apparent properties of oleogels.

3.6.2. X-ray diffraction (XRD)

XRD was used to recognize the crystalline characteristics of the oleogels. In Fig. 8, the XRD patterns of CNF powder and CNF-based oleogels were given for comparison. For CNF, three characteristic reflections at $2\theta = 16.10°$, 22.56° and 34.69° were observed, which could be attributed to the 10, 002 and 040 lattice planes of I-type cellulose (Fig. 8a). CNF showed the structure of semi-crystalline containing some amorphous regions, with the crystallinity degree of about 70.9%. Similar to previous researches in HPMC oleogels (Meng et al., 2018a; 2018c), the oleogels structured by CNF showed a single strong and broad peak at 2θ of around 19.6° (Fig. 8b, Table 1). The diffraction angle was slightly changed with the CNF loadings increasing from 0.4% to 4.0%, accompanied by the crystalline dimension decreasing slightly from 1.40 to 1.29 nm. The short spacing between crystalline planes was calculated as about 4.53 Å, which was the characteristic of typical β polymorph, a most stable polymorph with triclinic subcell arrangement, the highest packing density and the highest melting point (Co & Marangoni, 2020). This indicated relatively ordered network structure interfered by CNF, and was surely affected by the intermolecular non-covalent bonding between CNF factors with oil molecules during emulsion stage and after drying process.

3.6.3. FTIR spectra of oleogels

The molecular structures of CNF powder, walnut oil, and oleogels were analyzed by FTIR technology. The spectrum of CNF was displayed in Fig. 9a. The broad peak at around 3447.0 cm^{-1} was attributed to the stretching vibration of hydroxyl group in native cellulose. The minor peak at 2903.3 cm^{-1} corresponded to C–H stretching vibration of cellulose aliphatic function. The sharp peak at 1621.0 cm^{-1} was mainly due to C═O stretching vibration of -COONa, indicating the selective oxidation of primary hydroxyl group on anhydroglucose C6 atom (Wei et al., 2016). Peaks at 1423.6–1316.8 cm^{-1} originated from the in-plane bending of C–H and C–O linkages, while peaks around 1161.9–1035.2 cm^{-1} were resulted from the signal overlap of C–O stretching vibration and O–H association. The small peak at 898.7 cm^{-1} was probably the signal of anomeric carbon (C1) of glucose unit.

The spectrum of walnut oil was displayed in Fig. 9b. The small peak at 3009.1 cm^{-1} could be attributed to the C–H stretching of *cis*-olefinic bond, while two pointy peaks at 2926.2 and 2854.3 cm^{-1} corresponded to the asymmetrical and symmetrical stretching of methylene chain of fatty acids, respectively. The sharp peak at 1747.4 cm^{-1} indicated C═O stretching vibration of triacylglycerols, and that at 1654.3 cm^{-1} indicated the *cis*-olefinic C═C signal of unsaturated triacylglycerols. In fingerprint region of 1500–1000 cm^{-1}, peaks at 1464.4, 1397.3 and 1377.7 cm^{-1} were corresponding to the bending vibration of $-CH_2-$/$-CH_3$, *cis*-olefinic C–H and $-CH_2-$, respectively (Liang et al., 2013). Peaks at 1238.7, 1162.6, 1120.8 and 1099.6 cm^{-1} were possibly attributed to the characteristic absorption of C–O stretching vibration, while the peak at 723.0 cm^{-1} were the characteristic absorption of *cis*-olefinic C═C functionality (Wen et al., 2022).

FTIR spectra of the CNF-based oleogels were shown in Fig. 9c, which were similar to the spectrum of walnut oil. The peaks at around 3010.0, 2926.7, 2855.1, 1747.1, 1465.3, 1377.6, 1239.1, 1162.3, 1100.4 and 722.5 cm^{-1} were mainly attributed to the contributions from oil molecules, and were nearly unchanged. Remarkable frequency shifts after the gelation of walnut oil occurred at wavenumber range of 1720–1530 cm^{-1}. Peak at 1621.0 cm^{-1}, the signal of C═O stretching vibration of carboxyl group in CNF, was moved to wavenumber of around 1609.3 cm^{-1} for oleogels, with its intensity enhancing with the increase of CNF concentration in oleogels. Correspondingly, Peak at 1654.3 cm^{-1}, the signal of unsaturated C═C linkage of triacylglycerols, was shifted to wavenumber of around 1646.9 cm^{-1} for oleogels, with its intensity declining with the increase of CNF concentration. It implied that the carboxyl group of CNF gelator and the *cis*-olefinic functionality of oil solvent possibly involved in the gelation of walnut oil to a certain extent, although the detailed mechanism was still uncertain. The broad peak in the range of 3750–3050 cm^{-1} was mainly attributed to the contribution from hydroxyl group of CNF gelator. The wavenumber of this peak shifted up from 3352 cm^{-1} in the oleogel containing 0.4% CNF to 3567 cm^{-1} in the oleogel containing 4.0% CNF, which could be explained as stronger CNF-oil interactions at lower CNF concentration while stronger interactions between CNF molecules at higher concentration.

Table 1
XRD parameters of walnut oleogels with different CNF concentrations.

CNF concentration (%)	2θ (°)	Crystalline dimension D (Å)	Short spacing d (Å)
CNF powder	16.10, 22.56, 34.69	–	5.50, 3.94, 2.58
0.4	19.75	14.02	4.49
0.8	19.73	14.04	4.50
1.2	19.66	13.81	4.51
1.6	19.40	13.76	4.57
2.0	19.37	13.99	4.58
4.0	19.47	12.87	4.55

3.7. Oxidative stability of oleogels

The oxidative stability of oleogels stored at 37 °C was examined during 15 days at every 3 day intervals. The changes in POV and TBARS of walnut oil and its oleogels were shown in Fig. 10. The CNF oleogels with higher CNF concentrations (1.2%, 1.6%, 2.0% and 4.0%) revealed lower POV values than walnut oil ($p < 0.05$) after 9, 12, 15 days of storage (Fig. 10a), indicating that these oleogels possessed higher oxidative stability, and decreased the oxidation of susceptible liquid oil to peroxides or superoxides. The oleogels with higher CNF concentrations (1.6%, 2.0% and 4.0%) revealed lower TBARS value ($p < 0.05$) at the end of the experiment (15 days), when compared with walnut oil and the other oleogel samples in the same period of time (Fig. 10b), which indicated that the steric hindrance built by the dense gelation network added a protective barrier to the liquid oil and delayed the kinetic rate of oil molecules converting to secondary oxidation products like unpleasant aldehydes or ketones. Clearly, with the increasing concentration of CNF, a lower oxidation rate of the oleogels could be expected, which were attributed to the entrapped oil in the stronger network structure of the oleogels formed by CNF thereby retarding the oxidation by air (Kamali, Sahari, Barzegar, & Ahmadi Gavlighi, 2019). Similarly, the oxidative stability of rice bran wax-based walnut oleogel was significantly improved compared to liquid walnut oil, which structured *via* the aiding of soy protein isolate and phosphatidylserine (Yu et al., 2022).

4. Conclusions

Oleogels with different CNF concentrations (0.4, 0.8, 1.2, 1.6, 2.0 and 4.0%) were prepared by emulsion-templated method, and were evaluated for their structure and chemical properties. CNF concentration had a significant impact on the droplet size and stability of the O/W emulsions as the precursor of oleogels. The grape-like or disintegrated

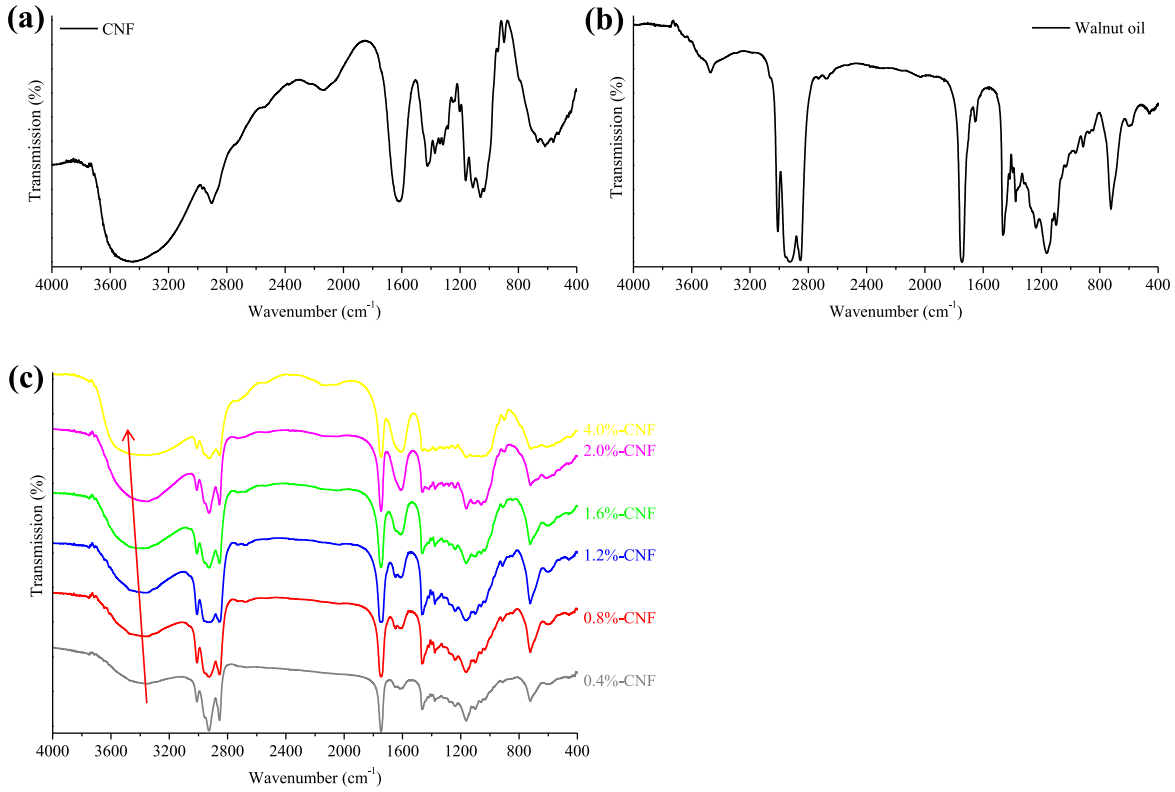

Fig. 9. FTIR spectra of CNF powder (a), walnut oil (b) and walnut oleogels with different CNF concentration (c).

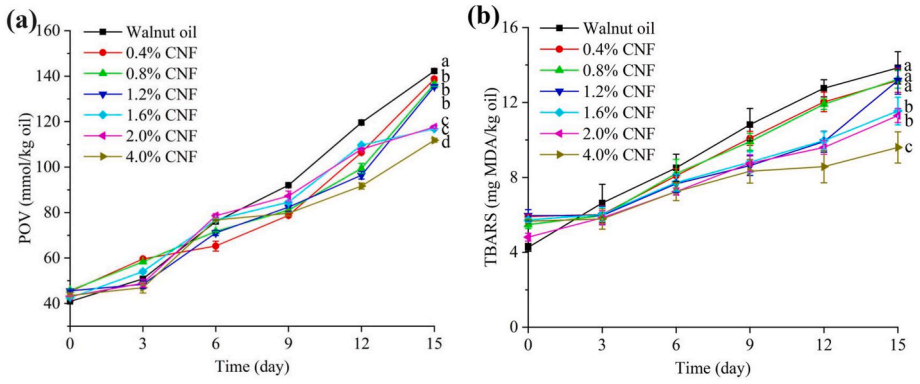

Fig. 10. POV values (A) and TBARS values (B) of walnut oil and walnut oleogels with different CNF concentrations during the storage period at 37 °C. a-d: different letters indicate significant differences ($p < 0.05$).

droplet cluster of emulsions at CNF concentration of higher than 1.0% provided high stability of emulsions after standing for 4 h at room temperature. At higher CNF loading (≥1.6%), the decreased droplet size and gradually disintegrated droplet cluster structure of O/W emulsion exerted obvious and positive influence on the oil-binding capacity (to >97%) and satisfactory stability of oleogels, as well as higher hardness, lower mobility and opaque appearance. The prepared oleogels possessed solid-like behaviors, with high gelation strength (G') of about 0.4-5.0 × 10^5 Pa, while the oxidation rate of walnut oil also remarkably decreased by at least 17% after walnut oil was gelated with 1.6–4.0% CNF. In conclusion, the CNF-based walnut oleogels prepared in this study show strengthened rheological and mechanical properties, as well as good thermal and oxidative stability, which provide potential feasibility for further application in functional foods.

Author contributions

Xiufen Li: Literature survey, Conceptualization, Manuscript preparation; **Guanshui Guo:** Investigation, Formal analysis; **Yuxuan Zou**: Formal analysis, Visualization; **Jia Luo**: Data curation, Writing-reviewing and editing; **Yang Tian** and **Jun Sheng**: Project administration, Writing-reviewing; **Jienan Li:** Methodology, resources.

Declaration of competing interest

The authors declare no competing financial interest.

Data availability

Data will be made available on request.

Acknowledgments

This research was financially supported by National Natural Science Foundation of China (32160564), Yunnan Fundamental Research Project (grant NO. 202001AU070106), Major Project of Science and Technology Department of Yunnan Province (202002AA100005 and 202102AE090027-2) and Cassava Industrial Technology System of China (CARS-11-YNTY).

References

Blake, A. I., Co, E. D., & Marangoni, A. G. (2014). Structure and physical properties of plant wax crystal networks and their relationship to oil binding capacity. *Journal of the American Oil Chemists' Society, 91*(6), 885–903.

Chu, Y., Sun, Y., Wu, W., & Xiao, H. (2020). Dispersion properties of nanocellulose: A review. *Carbohydrate Polymers, 250*, Article 116892.

Co, E. D., & Marangoni, A. G. (2020). Fat crystal networks (Vol. 1). In F. Shahidi (Ed.), *Bailey's industrial oil and fat products (Newly revised)*. John Wiley & Sons, Ltd.

Davidovich-Pinhas, M. (2019). Oil structuring using polysaccharides. *Current Opinion in Food Science, 27*, 29–35.

Davidovich-Pinhas, M., Gravelle, A. J., Barbut, S., & Marangoni, A. G. (2015). Temperature effects on the gelation of ethylcellulose oleogels. *Food Hydrocolloids, 46*, 76–83.

Espert, M., Salvador, A., & Sanz, T. (2020). Cellulose ether oleogels obtained by emulsion-templated approach without additional thickeners. *Food Hydrocolloids, 109*, Article 106085.

Foegeding, E. A., Bowland, E. L., & Hardin, C. C. (1995). Factors that determine the fracture properties and microstructure of globular protein gels. *Food Hydrocolloids, 9*(4), 237–249.

Foster, E. J., Moon, R. J., Agarwal, U. P., Bortner, M. J., Bras, J., Camarero-Espinosa, S., et al. (2018). Current characterization methods for cellulose nanomaterials. *Chemistry Society Reviews, 47*(8), 2609–2679.

Fujisawa, S., Togawa, E., & Kuroda, K. (2017). Nanocellulose-stabilized Pickering emulsions and their applications. *Science and Technology of Advanced Materials, 18*, 959–971.

Jiang, Y., Liu, L., Wang, B., Sui, X., Zhong, Y., Zhang, L., et al. (2018). Cellulose-rich oleogels prepared with an emulsion-templated approach. *Food Hydrocolloids, 77*, 460–464.

Kalogiouri, N. P., Manousi, N., Rosenberg, E., Zachariadis, G. A., Paraskevopoulou, A., & Samanidou, V. (2021). Exploring the volatile metabolome of conventional and organic walnut oils by solid-phase microextraction and analysis by GC-MS combined with chemometrics. *Food Chemistry, 363*, Article 130331.

Kamali, E., Sahari, M. A., Barzegar, M., & Ahmadi Gavlighi, H. (2019). Novel oleogel formulation based on amaranth oil: Physicochemical characterization. *Food Science and Nutrition, 7*(6), 1986–1996.

Liang, P. J., Chen, C. Y., Zhao, S. L., Ge, F., Liu, D. Q., Liu, B. Q., et al. (2013). Application of fourier transform infrared spectroscopy for the oxidation and peroxide value evaluation in virgin walnut oil. *Journal of Spectroscopy, 91*(6), 885–903.

Li, Q., Ma, Q., Wu, Y., Li, B., Luo, X., Liu, S., et al. (2020). Oleogel films through the pickering effect of bacterial cellulose nanofibrils featuring interfacial network stabilization. *Journal of Agricultural and Food Chemistry, 68*, 9150–9157.

Lu, Y., Li, J., Ge, L., Xie, W., & Wu, D. (2021). Pickering emulsion stabilized with fibrous nanocelluloses: Insight into fiber flexibility-emulsifying capacity relations. *Carbohydrate Polymers, 255*, Article 117483.

Lu, Y., Qian, X., Xie, W., Zhang, W., Huang, J., & Wu, D. (2019). Rheology of the sesame oil-in-water emulsions stabilized by cellulose nanofibers. *Food Hydrocolloids, 94*, 114–127.

McClements, D. J. (2020). Future foods: A manifesto for research priorities in structural design of foods. *Food & Function, 11*(3), 1933–1945.

Mendoza, L., Batchelor, W., Tabor, R., & Garnier, G. (2018). Gelation mechanism of cellulose nanofibre gels: A colloids and interfacial perspective. *Journal of Colloid and Interface Science, 509*, 39–46.

Meng, Z., Qi, K., Guo, Y., Wang, Y., & Liu, Y. (2018a). Macro-micro structure characterization and molecular properties of emulsion-templated polysaccharide oleogels. *Food Hydrocolloids, 77*, 17–29.

Meng, Z., Qi, K., Guo, Y., Wang, Y., & Liu, Y. (2018b). Physical properties, microstructure, intermolecular forces, and oxidation stability of soybean oil oleogels structured by different cellulose ethers. *European Journal of Lipid Science and Technology, 120*, Article 1700287.

Meng, Z., Qi, K., Guo, Y., Wang, Y., & Liu, Y. (2018c). Effects of thickening agents on the formation and properties of edible oleogels based on hydroxypropyl methyl cellulose. *Food Chemistry, 246*, 137–149.

Metin, S., & Hartel, R. W. (2020). Fundamentals of lipid crystallization (Vol. 1). In F. Shahidi (Ed.), *Bailey's industrial oil and fat products (Newly revised)*. John Wiley & Sons, Ltd.

Ostertag, F., Weiss, J., & McClements, D. J. (2012). Low-energy formation of edible nanoemulsions: Factors influencing droplet size produced by emulsion phase inversion. *Journal of Colloid and Interface Science, 388*, 95–102.

Pan, H., Xu, X., Qian, Z., Cheng, H., Shen, X., Chen, S., et al. (2021). Xanthan gum-assisted fabrication of stable emulsion-based oleogel structured with gelatin and proanthocyanidins. *Food Hydrocolloids, 115*, Article 106596.

Patel, A. R., Rodriguez, Y., Lesaffer, A., & Dewettinck, K. (2014). High internal phase emulsion gels (HIPE-gels) prepared using food-grade components. *RSC Advances, 4*, Article 18136.

Pehlivanoglu, H., Demirci, M., Toker, O. S., Konar, N., Karasu, S., & Sagdic, O. (2018). Oleogels, a promising structured oil for decreasing saturated fatty acid concentrations: Production and food-based applications. *Critical Reviews in Food Science and Nutrition, 58*(8), 1330–1341.

Pernetti, M., van Malssen, K. F., Flöter, E., & Bot, A. (2007). Structuring of edible oils by alternatives to crystalline fat. *Current Opinion in Colloid & Interface Science, 12*, 221–231.

Perumal, B. A., Nambiar, R. B., Moses, J. A., & Anandharamakrishnan, C. (2022). Nanocellulose: Recent trends and applications in the food industry. *Food Hydrocolloids, 127*, Article 107484.

Phoon, P. Y., & Henry, C. J. (2020). Fibre-based oleogel: Effect of the structure of insoluble fibre on its physical properties. *Food & Function, 11*, 1349–1361.

Rebufa, C., Artaud, J., & Dreau, Y. L. (2022). Walnut (*Juglans regia* L.) oil chemical composition depending on variety, locality, extraction process and storage conditions: A comprehensive review. *Journal of Food Composition and Analysis, 110*, Article 104534.

Shao, P., Feng, J., Sun, P., Xiang, N., Lu, B., & Qiu, D. (2020). Recent advances in improving stability of food emulsion by plant polysaccharides. *Food Research International, 137*, Article 109376.

Shen, W., Guo, L., Wu, T., Zhang, W., & Abid, M. (2016). Stabilizing beverage emulsions by regenerated celluloses. *LWT-Food Science and Technology, 72*, 292–301.

Sun, H., Xu, J., Lu, X., Xu, Y., Regenstein, J. M., Zhang, Y., et al. (2022). Development and characterization of monoglyceride oleogels prepared with crude and refined walnut oil. *LWT - Food Science and Technology, 154*, Article 112769.

Wang, L., Wen, Y., Su, C., Gao, Y., Li, Q., Du, S., et al. (2022). Effect of water content on the physical properties and structure of walnut oleogels. *RSC Advances, 12*, 8987.

Wei, J. G., Chen, Y. F., Liu, H. Z., Du, C. G., Yu, H. L., & Zhou, Z. X. (2016). Thermo-responsive and compression properties of TEMPO-oxidized cellulose nanofiber-modified PNIPAm hydrogels. *Carbohydrate Polymers, 147*, 201–207.

Wen, Y. X., Zhou, S., Wang, L. Q., Li, Q., Gao, Y., & Yu, X. Z. (2022). New method for the determination of the induction period of walnut oil by fourier transform infrared spectroscopy. *Food Analytical Methods, 15*, 833–843.

Xu, J., Sun, H., Zhang, G., & Wang, J. (2020). Preparation and properties of walnut oil-based oleogels. *Food and Fermentation Industries, 46*(5), 188–193.

Yu, Y., Wang, T., Gong, Y., Wang, W., Wang, X., Yu, D., et al. (2022). Effect of ultrasound on the structural characteristics and oxidative stability of walnut oil oleogel coated with soy protein isolate-phosphatidylserine. *Ultrasonics Sonochemistry, 83*, Article 105945.